Lipophilic Hexadentate Gallium, Indium and Iron Complexes of New Phenolate-derivatized Cyclohexanetriamines as Potential *in vivo* Metal-transfer Reagents†

James E. Bollinger,[a] Joel T. Mague, [a] Charles J. O'Connor,[b] William A. Banks[c] and D. Max Roundhill*,[a]

[a] *Department of Chemistry, Tulane University, New Orleans, Louisiana 70118, USA*
[b] *Department of Chemistry, University of New Orleans, New Orleans, Louisiana 70148, USA*
[c] *Veterans Affairs Medical Center and Tulane University School of Medicine, 1601 Perdido Street, New Orleans, Louisiana 70146, USA*

1,3,5-Tris(5-substituted salicylamino)cyclohexanes (H_3L; R = H, NO_2 or OMe) have been synthesized by Schiff-base condensation between *cis*-1,3,5-triaminocyclohexane and a substituted salicylaldehyde, followed by reduction with KBH_4. Reaction of these compounds with gallium(III), indium(III) and iron(III) salts gave neutral six-co-ordinate N_3O_3 complexes of type [ML] (M = Ga, In or Fe). The complexes have been characterized by a combination of infrared, ^1H and ^{13}C-{^1H} NMR and mass spectroscopy. The distribution coefficients between octan-1-ol and water indicate that the complexes are lipophilic. The electronic absorption spectra of the high-spin iron(III) complexes show ligand-to-metal charge-transfer bands in the 450–500 nm range. The structures of five of the complexes have been confirmed by single-crystal X-ray crystallography.

Owing to the clinical importance of trivalent metal ions there is a need to synthesize chelating agents which are specifically designed for such applications.[1] There are, however, a number of restrictions that must be met. Among these is the requirement that generally both the free chelator and its complexes should be water soluble. Nevertheless, if the agent is to be used to scavenge a metal ion *in vivo* it must be able to penetrate cell membranes. As a result it cannot possess charged functional groups in solutions having physiological pH, and the resulting complexes must also be neutral. Neutral chelating agents are also more likely to be orally active and, if their molecular weight is less than 400, they may penetrate the blood–brain barrier.

In addition to the aforementioned requirements it is also important that the metal be tightly bound within the chelate ligand. With kinetically labile complexes the metal may be donated to endogenous high-affinity binding sites such as those located on the plasma protein apotransferrin. In order to obtain kinetically inert complexes it is usually advantageous to use multidentate chelating agents. In general, oligodentate chelates are more kinetically inert than are bidentate ones. Two important applications of trivalent metal ions are in iron scavenging and in imaging. For magnetic resonance imaging with gadolinium(III), chelating agents that can accommodate high co-ordination numbers are preferable. One of the reasons that six-co-ordinate complexes of the Group 13 (IIIB) metal ions are of biomedical interest, however, is because of the potential use of gallium and indium radioisotopes for imaging applications.[2–5] The isotopes ^{67}Ga, ^{68}Ga, ^{111}In and ^{113}In have the appropriate energies and half-lives for either γ-scintigraphy or positron emission tomography.[6–8] High binding constants for these metal ions are generally found with multidentate 'hard' ligands, and in particular the phenolate anion is a strongly co-ordinating moiety.[9–13] Although there are many examples of ethylenediamine-*N*,*N*,*N*′,*N*′-tetraacetate (edta) and polyazacarboxylate complexes with gallium(III) and indium(III),[14–28] there are somewhat fewer cases where a multidentate phenolate moiety has been used as a complexant for these ions.[29–40] Since gallium(III) and indium(III) preferentially form octahedral complexes, our choice of chelating agent is one that has three phenolate groups appended to a *cis*-cyclohexanetriamine backbone.[41–44] These ligands with N_3O_3 co-ordination resemble similar ones based on a macrocyclic or a pyramidal backbone.[45,46] They have been designed to avoid the presence of C=N functional groups because it is believed that such groups undergo degradation under *in vivo* conditions.[47] If gallium(III) and indium(III) complexes are to be used as myocardial perfusion agents, it is preferable that they be overall neutral and lipophilic.[48] Such a situation can be achieved with trianionic ligands that can have a range of different substituents appended to their periphery.

The gradual accumulation of iron is associated with a number of diseases such as β-thalassaemia.[49] It is important therefore to develop chelators that can be used to reduce iron overload and the health effects associated with it. In addition chelators may also be useful for the treatment of inflammatory diseases such as rheumatoid arthritis through their action as scavengers for iron.[1] In microorganisms the iron-complexing compounds that are secreted are the siderophores. These chelating agents typically have hydroxamate or catecholate groups that co-ordinate to the Fe^{3+} centre, therefore these functionalities are preferred ones for forming stable complexes of this ion.[50–52] Since the co-ordination properties of Ga^{3+} and Fe^{3+} are very similar, we have incorporated phenolic groups into the chosen ligands. We report here the synthesis and characterization of a new set of uncharged chelating agents, 1,3,5-tris(5-substituted salicylamino)cyclohexanes (R = H, NO_2 or OMe), and their six-co-ordinate complexes of trivalent gallium, indium and iron. These complexes meet many of the necessary criteria for potential use in clinical applications, although phenolate groups are protonated under acidic conditions.[20]

Experimental

Preparations and Measurements.—All materials and solvents were standard reagent grade used without further purification unless otherwise noted. Reagents were obtained from Aldrich

† *Supplementary data available:* see Instructions for Authors, *J. Chem. Soc., Dalton Trans.*, 1995, Issue 1, pp. xxv–xxx.

Chemical Co., with the exceptions of diethylene glycol (Eastman) and sodium triazide (Alfa). The salts $In(ClO_4)_3 \cdot 8H_2O$ (Aesar), $Ga(ClO_4)_3 \cdot 6H_2O$ (Johnson Matthey) and $Fe(NO_3)_3 \cdot 9H_2O$ (J. T. Baker) were all >99% pure (metals basis) and were used without further purification. Melting points, where appropriate, were obtained on a hot-stage apparatus. Infrared spectra were recorded as KBr pellets using a Mattson Cygnus 100 FT-IR spectrometer, electronic spectra (as acetonitrile solutions unless otherwise noted) with a Hewlett-Packard model 8451 diode-array spectrophotometer, ^1H and ^{13}C NMR spectra using a GE Omega 400 MHz instrument (unless otherwise noted) and fast atom bombardment (FAB) mass spectra by means of a Kratos Concept 1H spectrometer with the samples introduced in a *m*-nitrobenzyl alcohol matrix. Elemental analyses were performed by Galbraith Inc., Knoxville, TN.

cis-1,3,5-*Tris*(*phenylsulfonyloxy*)*cyclohexane*.—*cis*-Cyclohexane-1,3,5-triol dihydrate (6.85 g, 40.7 mmol) was dissolved in freshly distilled pyridine (90 cm^3). This solution was maintained at 10 °C while benzenesulfonyl chloride (53 g, 0.3 mol) was added over a period of 3 h. The resulting mixture formed a thick off-white slurry. This was added to a solution of water (175 cm^3), ethanol (350 cm^3) and concentrated HCl (140 cm^3), and stirred for 30 min. The resulting white solid was filtered off and washed with ethanol. The product was purified by recrystallization by addition of ethanol (1.5 l), heating to reflux, and addition of sufficient dichloromethane to complete dissolution. After cooling the product formed as fine colourless needles.[53] Yield: 18.6 g, 35.6 mmol (87.4%). M.p. 189 °C (decomp.). ^1H NMR [$(CD_3)_2SO$]: δ 1.61 [q, 3 H, $^3J(HH)$ = 12], 1.71 (m, 3 H), 4.49 (m, 3 H), 7.62 [t, 6 H, $^3J(HH)$ = 8], 7.77 [d, 6 H, $^3J(HH)$ = 8] and 7.79 [t, 3 H, $^3J(HH)$ = 8 Hz].

cis-1,3,5-*Triazidocyclohexane*.—*cis*-1,3,5-Tris(phenylsulfonyloxy)cyclohexane (18.6 g, 35.6 mmol) was placed in a flask (250 cm^3) equipped with a thermometer and magnetic stirrer. To this solid was added diethylene glycol (70 cm^3) and sodium azide (11.6 g, 178 mmol). After stirring this mixture at 100 °C for 6 h the solution had turned a clear light brown. After the solution had cooled to room temperature it was poured into water (140 cm^3) and stirred for a few minutes. Dichloromethane–tetrahydrofuran (thf) (50:50 v/v, 60 cm^3) was added and the stirring continued for 15 min. This mixture was allowed to stand and the layers separated. The aqueous layer was extracted with CH_2Cl_2–thf (50:50 v/v, 2 × 50 cm^3). The combined organic fractions were washed with water (1 × 50 cm^3 portion), decolorized and dried over $MgSO_4$. After removal of the solvent a clear light tan oil was obtained. Yield: 5.8 g, 28 mmol (79%). ^1H NMR [$(CD_3)_2SO$]: δ 1.28 [q, $^3J(HH)$ = 12], 2.16 [dt, $^3J(HH)$ = 11, 4] and 3.53 [td, $^3J(HH)$ = 12, 4 Hz]. **CAUTION:** polyazides are potentially explosive!

cis-1,3,5-*Triaminocyclohexane Trihydrochloride* (tach·3HCl).—*cis*-1,3,5-Triazidocyclohexane (5.8 g, 28 mmol) in freshly distilled thf (40 cm^3) was added to a rapidly stirred mixture of $LiAlH_4$ (4.7 g, 0.12 mol) in freshly distilled thf (40 cm^3) over a period of 2 h under nitrogen. After addition was complete the mixture was refluxed for 18 h. After cooling, water (5 cm^3) was added followed by NaOH (5 cm^3 of 15% aqueous solution) and water (15 cm^3). The resulting slurry was filtered through a Soxhlet thimble and continuously extracted with a mixture of the supernatant and thf for 12 h. The solvent was removed under reduced pressure to give a nearly colourless oil. The crude product was taken up in EtOH (250 cm^3) and any insoluble material filtered off. To this stirred solution was added dropwise concentrated HCl (8 cm^3) to precipitate the compound as the tris(hydrochloride) salt. The product was purified by dissolution in water (150 cm^3), filtered, and made basic (pH 12) by addition of NaOH. The solvent was then removed on a rotary evaporator. The product was reprecipitated from an EtOH solution as a fine white powder. Yield: 4.84 g, 20.3 mmol (72%). ^1H NMR [$(CD_3)_2SO$]: δ 1.48 [q, 3 H, $^3J(HH)$ = 12], 2.31 [d, 3 H, $^3J(HH)$ = 12 Hz], 3.21 (m, 3 H) and 8.52 (br s, 9 H).

cis-1,3,5-*Tris*(*salicylideneamino*)*cyclohexane*.—The compound tach·3HCl (2.0 g, 8.4 mmol) was dissolved in water (50 cm^3) and NaOH pellets added (1.0 g). The solvent was removed under reduced pressure on a rotary evaporator. To the resulting residue was added absolute ethanol (20 cm^3). The mixture was sonicated for 5 min, then allowed to stand at 5 °C for 1 h, and filtered. Salicylaldehyde (*o*-hydroxybenzaldehyde) (4.5 g, 37 mmol) was added to the supernatant and the mixture refluxed for 20 min and cooled to 5 °C. The yellow precipitate was filtered off and washed with cold ethanol. If discoloration occurred the solid was refluxed in water (75 cm^3) for 15 min. The reaction mixture was cooled and filtered to yield the product as a yellow microcrystalline powder.[54] Yield: 3.3 g, 7.4 mmol (88%). ^1H NMR [$(CD_3)_2SO$, 200 MHz]: δ 1.72 [q, 3 H, $^3J(HH)$ = 12], 2.04 (m, 3 H), 3.70 (m, 3 H), 6.89 [t, 6 H, $^3J(HH)$ = 8], 7.33 [t, 3 H, $^3J(HH)$ = 6], 7.45 [d, 3 H, $^3J(HH)$ = 8 Hz], 8.67 (s, 3 H) and 13.42 (s, 3 H).

cis-1,3,5-*Tris*(*salicylamino*)*cyclohexane* (H_3tstach).—The above compound (3.3 g, 7.4 mmol) was added to a mixture of borax ($Na_2B_4O_7 \cdot 10H_2O$ 1.4 g, 7.0 mmol), in absolute ethanol (200 cm^3) under nitrogen. The salt KBH_4 (1.5 g, 28 mmol) was slowly added with stirring. The mixture was stirred for 12 h at ambient temperature and refluxed for 3 h after which time it had become clear and light brown. Water (20 cm^3) was stirred into the solution and the mixture filtered. To the supernatant was added ammonium chloride (12 g) in water (80 cm^3) to give a white precipitate. The product was purified by recrystallization from a mixture of water and thf. Yield: 2.4 g, 5.4 mmol (73%).

cis-1,3,5-*Tris*(5-*nitrosalicylideneamino*)*cyclohexane*.—The preparation of this derivative was similar to that of the unsubstituted salicylidene compound. The compound tach·3HCl (2.00 g, 8.4 mmol) was neutralized and dissolved in a minimum of absolute ethanol. To this solution was added 5-nitrosalicylaldehyde (4.9 g, 29 mmol) along with sufficient ethanol to increase the solution volume to 100 cm^3. This mixture was refluxed for 3 h during which time it thickened and changed from yellow to green-yellow. It was cooled to 5 °C, filtered and rinsed with ethanol (3 × 10 cm^3) to yield the product as a yellow powder. Yield: 4.2 g, 7.3 mmol (87%). M.p. 305 °C (decomp.). IR (KBr pellet): $\tilde{\nu}_{max}/cm^{-1}$ 3097w, 3055w, 1670s, 1604s and 1327s. ^1H NMR [$(CD_3)_2SO$]: δ 1.92 [q, 3 H, $^3J(HH)$ = 12], 2.28 (m, 3 H), 3.93 (m, 3 H), 6.82 [d, 3 H, $^3J(HH)$ = 10], 8.11 [dd, 3 H, $^3J(HH)$ = 9, $^5J(HH)$ = 3], 8.50 [d, 3 H, $^5J(HH)$ = 3 Hz] and 8.87 (s, 3 H).

cis-1,3,5-*Tris*(5-*nitrosalicylamino*)*cyclohexane* (H_3tnstach).—The preparation of this compound was similar to that of the unsubstituted salicyl derivative except that the above compound (4.2 g, 7.3 mmol) was used in a solution volume of 200 cm^3. The mixture was refluxed after the addition of borax and KBH_4 for a total of 6 h. Upon heating it became clear orange followed by formation of a yellow precipitate. After the mixture had cooled to ambient temperature water (50 cm^3) was added and the solution stirred for 0.5 h and filtered. To the supernatant was added ammonium chloride (14 g) in water (80 cm^3) causing the formation of a yellow precipitate. The mixture was refrigerated and filtered, the solid washed with water (2 × 10 cm^3) then ethanol (2 × 10 cm^3). The crude yield was 3.4 g, 6.3 mmol (86%). This compound was purified *via* the hydrochloride salt. The crude product was suspended in

a mixture of water (60 cm^3) and ethanol (60 cm^3), and concentrated HCl (20 cm^3) was added dropwise. Recrystallization from the same solvent system yielded the product as a fine crystalline powder.

cis-1,3,5-*Tris*(5-*methoxysalicylideneamino*)*cyclohexane*.—The compound tach·3HCl (2.00 g, 8.4 mmol) was neutralized by dissolution in water followed by passage of the solution through a Dowex anion-exchange column (1.5 × 15 cm) in its hydroxy form. The solvent was removed on a rotary evaporator and the resulting amine dissolved in absolute ethanol (100 cm^3). To this solution was added 5-methoxysalicylaldehyde (4.6 g, 30 mmol) and the mixture stirred until a yellow precipitate formed. This mixture was refluxed for 1 h, cooled to 5 °C, filtered and rinsed with ethanol (3 × 10 cm^3) to yield the product as a yellow powder. Yield: 3.9 g, 7.4 mmol (88%). IR (KBr pellet): $\tilde{\nu}_{max}/cm^{-1}$ 2937w, 2831w, 1639s, 1587s, 1491s, 1462m and 1276s. ^1H NMR [$(CD_3)_2SO$, 400 MHz]: δ 1.75 [q, 3 H, $^3J(HH) = 12$], 1.98 (m, 3 H), 3.67 (m, 3 H), 3.68 (s, 9 H), 6.80 [d, 3 H, $^3J(HH) = 9$], 6.93 [dd, 3 H, $^3J(HH) = 9$, $^5J(HH) = 3$], 7.04 [d, 3 H, $^5J(HH) = 3$ Hz], 8.61 (s, 3 H) and 12.77 (s, 3 H).

cis-1,3,5-*Tris*(5-*methoxysalicylamino*)*cyclohexane* (H_3tmstach).— The above compound (3.9 g, 7.4 mmol) was dissolved in absolute ethanol (150 cm^3) to give a saturated solution. To this mixture was added borax (1.4 g, 7.0 mmol), and after stirring for 15 min KBH_4 (1.5 g, 28 mmol) was added slowly. The stirring was continued for 30 min under nitrogen, the mixture refluxed for 1 h, and then stirred at ambient temperature for 12 h. The suspension became colourless. The mixture was decanted from the borax and water (20 cm^3) was added dropwise under nitrogen. Ammonium acetate (12 g) in water (80 cm^3) was added. The mixture was cooled to 5 °C and filtered to yield the product as a cream powder. Yield: 3.5 g, 6.5 mmol (88%).

Synthesis of Metal Complexes.—In all cases the preparations described are on a small scale (< 100 mg) and were conducted in round-bottomed or Schlenk flasks (100 cm^3) under nitrogen. All metal salts, excluding iron, were stored and weighed in a dry-box under an inert atmosphere before use. All metal complexes have decomposition temperatures greater than 280 °C. Analytical and mass spectral data for the complexes are given in Table 1, infrared, UV/VIS, ^1H and ^{13}C-{^1H} NMR spectral data in Tables 2–5.

[Fe(tstach)]. The compound H_3tstach (0.1 g, 0.22 mmol) was added to dry methanol (50 cm^3) and stirred until the maximum quantity of solute had dissolved. The salt $Fe(NO_3)_3 \cdot 9H_2O$ (0.090 g, 0.22 mmol) was dissolved separately in methanol (5 cm^3) and the solution allowed to stand over molecular sieves (3 Å type) for 15 min. This solution was added dropwise to the stirred solution of H_3tstach to give a deep violet solution. After 15 min ethyldiisopropylamine (1 cm^3) was added dropwise and the mixture refluxed for 12 h. After this time the solution had become clear, rust red. The solvent volume was reduced to 5 cm^3 on a rotary evaporator and water (25 cm^3) added to produce a dark maroon precipitate. The solid was filtered off, washed with water (3 × 5 cm^3), and dried in a vacuum oven for 1 d. Yield: 0.10 g, 0.20 mmol (91%).

[Ga(tstach).] A similar procedure was followed except in the use of $Ga(ClO_4)_3 \cdot 6H_2O$ (0.10 g, 0.22 mmol). The purification procedure involved taking up the residue in CH_2Cl_2–MeOH (90:10 v/v, 4 cm^3) followed by flash chromatography (silica gel, 325 mesh, 15 × 1.5 cm column) in the same mixed solvent. The solvent was removed to give the product as a nearly colourless powder. Yield: 0.84 g, 0.17 mmol (75%).

[In(tstach)]. The synthetic method used was similar to that for the corresponding gallium complex except in the use of $In(ClO_4)_3 \cdot 8H_2O$ (0.12 g, 0.22 mmol). The purification was conducted in a manner identical to that for [Ga(tstach)] to give the product as a nearly colourless powder. Yield 0.095 g, 0.17 mmol (78%).

[Fe(tnstach)]. The compound H_3tnstach·3HCl·$3H_2O$ (0.16 g, 0.22 mmol) was dissolved in absolute ethanol (50 cm^3). To this mixture was added a solution of $Fe(NO_3)_3 \cdot 9H_2O$ in ethanol (4 cm^3) which had been dried with molecular sieves as for the preparation of [Fe(tstach)]. This addition caused dissolution and a colour change to deep red. While the solution was rapidly stirred, ethyldiisopropylamine (1.5 cm^3) was added dropwise to give a red flocculate. This mixture was refluxed for 12 h after which time a brick-red precipitate had formed. The mixture was cooled to 4 °C and the precipitate filtered off to give the product as a fine powder. Yield: 0.13 g, 0.21 mmol (98%).

[Ga(tnstach)]. The preparative procedure was similar to those for the respective iron complexes except in the use of $Ga(ClO_4)_3 \cdot 6H_2O$ (0.10 g, 0.22 mmol). Filtration of the resulting precipitate yielded the product as a fine orange-yellow powder. Yield: 0.11 g, 0.20 mmol (90%).

[In(tnstach)]. The preparation was similar to that for the respective iron complex except in the use of $In(ClO_4)_3 \cdot 8H_2O$ (0.12 g, 0.22 mmol). Filtration of the resulting precipitate yielded the product as a fine yellow powder. Yield: 0.12 g, 0.20 mmol (90%).

[Fe(tmstach)]. The compound H_3tmstach (0.12g, 0.22 mmol) was dissolved in absolute ethanol (50 cm^3) to give a saturated solution. The salt $Fe(NO_3)_3 \cdot 9H_2O$ (0.089 g, 0.22 mmol) in ethanol (4 cm^3) was dried over molecular sieves as previously described and added to the stirred mixture to effect a colour change to deep purple. To this solution was added ethyldiisopropylamine (1 cm^3) dropwise. The solution was refluxed for 12 h after which time the solvent was removed on a rotary evaporator. The resulting residue was placed in a vacuum oven at 0.3 atm (*ca.* 3 × 10^4 Pa) and 100 °C for 12 h to remove the excess of amine. The crude product was dissolved in a small volume of methanol–dichloromethane (10:90 v/v) and purified by flash chromatography using these solvents in the same proportions (1.5 × 30 cm column, R_f = 0.4).

[Ga(tmstach)]. Except for the use of $Ga(ClO_4)_3 \cdot 6H_2O$ (0.10 g, 0.22 mmol), the procedure was identical to that for the iron complex. The purification procedure differed in that an alumina column (Brockman type I, neutral, 2 × 15 cm) was used, and the complex was eluted with methanol–dichloromethane (15:85 v/v). Fractions were assayed on silica TLC plates using the same solvent mixture (R_f = 0.5). Subsequent removal of the solvent on a rotary evaporator yielded the complex as a yellow powder.

[In(tmstach)]. Except for the use of $In(ClO_4)_3 \cdot 8H_2O$ (0.12 g, 0.22 mmol), the synthesis and purification were identical to those used for the gallium complex. The complex was obtained as a light yellow powder.

Alternate Method. An alternate synthetic method for the complexes used the same metal and ligand proportions except that anhydrous metal chlorides were employed and dissolved in solvent (2–4 cm^3), without the use of molecular sieves. The solvents were the same as described in the previous method except that diethylamine (1 cm^3) was used in place of ethyldiisopropylamine. Mixtures were then refluxed for 12 h under nitrogen. The crude product was purified as described previously.

Partition Coefficients.—Octanol–water partition coefficients were determined for the complexes by dissolving a small amount (*i.e.* the tip of a microspatula) of material as completely as possible in octanol (10 cm^3) in a screw-cap vial (25 cm^3). To this vial was added deionized water (10 cm^3). The mixture was stirred for 18 h at a rate that avoided emulsification. The mixture was allowed to stand overnight and was poured into a separation funnel (60 cm^3), and the two layers separated. For analysis the layers were centrifuged or filtered through a Gooch crucible if needed to remove any particulates. The samples were diluted as necessary such that the primary absorption in their UV/VIS spectra was < 0.5. The corrected absorption values

were then compared directly between octanol and water layers and expressed as the given ratios. These data are collected in Table 6.

Magnetic Susceptibility Data.—Magnetic susceptibility data were recorded over a temperature range of 10–300 K at a measuring field of 2.0 kOe (2×10^6 A m^{-1}) with an SHE Corp. VTS-50 superconducting SQUID susceptometer interfaced to an IBM XT computer system. Calibration and operating procedures have been reported elsewhere.[55]

X-Ray Data Collection and Structure Determination.—Red crystals of [Fe(tstach)]·3H_2O were grown by the slow diffusion of water into a dimethyl sulfoxide (dmso) solution of the complex, red crystals of [Fe(tnstach)]·EtOH by slow diffusion of ethanol into a dimethylformamide solution of the complex, dark violet crystals of [Fe(tmstach)] by slow evaporation from an acetone solution of the complex and crystals of [Ga(tstach)]·3.5H_2O and [In(tstach)]·3.5H_2O by slow diffusion of water into a dmso solution of the complex. The crystals were trimmed to size and mounted on thin glass fibres with a thin coat of epoxy cement. X-Ray diffraction data were collected on an Enraf-Nonius CAD-4 diffractometer. Cell constants and an orientation matrix for the data collection were obtained from the diffractometer routines from approximately 25 reflections. Equivalent reflections were merged, and data were corrected for Lorentz and polarization factors. Structures were solved using previously described techniques.[56–59] Selected bond distances and angles are collected in Table 7. Crystallographic details are summarized in Table 8, positional parameters are given in Tables 9–13, and ORTEP[60] representations in Figs. 2–6 respectively.

Additional material available from the Cambridge Crystallographic Data Centre comprises thermal parameters and remaining bond lengths and angles.

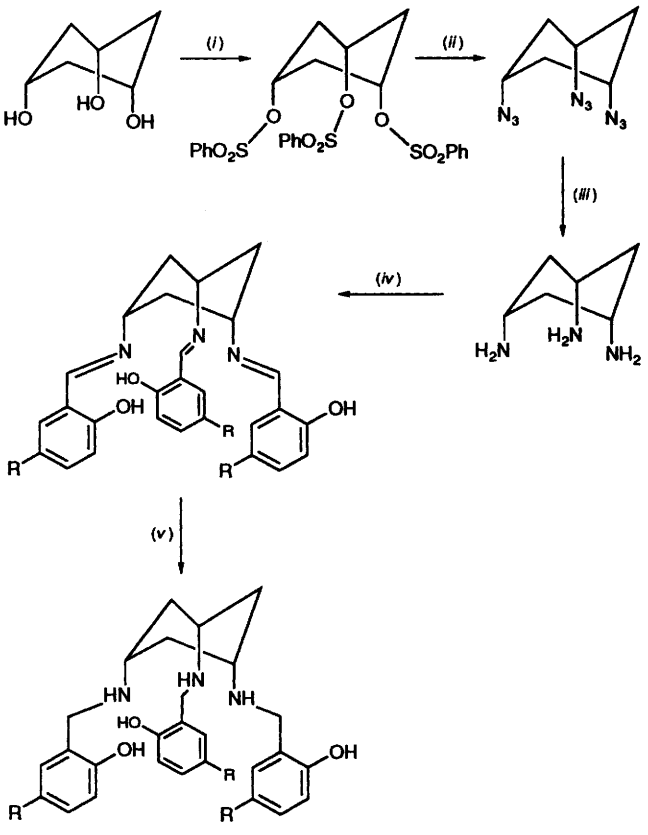

Scheme 1 (*i*) PhO_2SCl, pyridine, 10 °C; (*ii*) NaN_3, diethylene glycol, 100 °C; (*iii*) $LiAlH_4$, thf, reflux; (*iv*) salicylaldehyde, (R = H); 5-nitrosalicylaldehyde, (R = NO_2) or 5-methoxysalicylaldehyde (R = OMe), EtOH, reflux; (*v*) KBH_4, EtOH, reflux

Results

The three chelating agents that have been used in this study are as shown in Scheme 1. They have the *cis* stereochemistry about the cyclohexane ring, and the phenolic groups are appended in an arrangement whereby the deprotonated phenolate derivatives can readily give neutral hexadentate complexes with trivalent metal ions. In their deprotonated forms these compounds are abbreviated as tstach (R = H), tnstach (R = NO_2) and tmstach (R = OMe). The three R substituents have been chosen to offer different electronegativity and lipophilicity characteristics to the complexes. By comparison with the derivative having R = H, the NO_2 group is more electron withdrawing and the OMe group is more electron donating. Also, whereas the NO_2 group can be anticipated to offer a greater hydrophilicity to a complex than a hydrogen, the OMe group may offer a slight increase in hydrophobicity.

The phenolate-derivatized cyclohexanetriamine ligands have been synthesized by the procedure shown. This route was chosen from *cis*-cyclohexane-1,3,5-triol because we found it to be the most reliable for synthesizing *cis*-1,3,5-triaminocyclohexane. An alternate one-step literature procedure to this triamine from phloroglucinol was initially followed, but we found that the yields of product obtained were consistently very low.[43] Schiff-base condensation between *cis*-1,3,5-triaminocyclohexane and either salicylaldehyde or a substituted salicylaldehyde gives the unsaturated imine from which the saturated C–N derivative is obtained by reduction with potassium tetrahydroborate. In addition to designing a chelating agent with the preferred co-ordination and lipophilicity characteristics, it has been chosen to have fully saturated bonds between carbon and nitrogen because unsaturated C=N bonds are considered to be a cleavage point for biodegradation under *in vivo* conditions.

Metal Complexes.—Complexes of the trivalent gallium, indium and iron ions with these chelators have been synthesized by treating salts of these ions with a 1:1 stoichiometric ratio of the chelator H_3L in methanol solvent (Scheme 2). In all cases the yield was >75%. The stoichiometry of the uncharged complex has been confirmed by a combination of microanalytical and mass spectroscopic (FAB) techniques (Table 1). In each case a peak for the parent ion is observed in the mass spectrum. The infrared spectra show bands due to phenyl-group bending modes, and to ν(NH) in the 3200–3300 cm^{-1} range. For the complexes of tnstach two additional bands due to $\nu(NO_2)$ are found in the 1300–1500 cm^{-1} range and for the complexes of tmstach a band due to ν(CH) of the methoxy group is observed at 2900–3000 cm^{-1}. Complexation *via* the amine nitrogen is supported by the observation that both ν(NH) and δ(NH) are shifted to lower energy when compared to the free chelator.

The gallium and indium complexes are colourless, whereas the iron complexes are red. The electronic absorption spectra of the gallium and indium complexes show two bands in the UV region, whereas the spectra of the iron complexes show three bands (Table 3). The third band of the iron complexes is at longer wavelength than those of the other two bands. If we assign the last two to π–π* transitions primarily centred on the aromatic groups of the ligands, the third band can be assigned

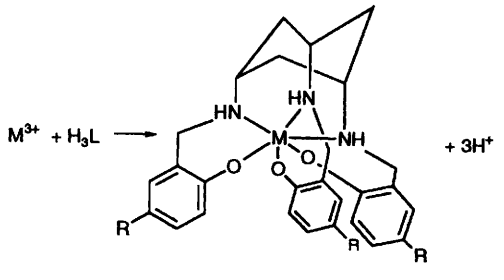

Scheme 2 M = Ga, In or Fe; R = H, NO_2 or OMe

Table 1 Analytical data (calculated in parentheses) for the complexes

	Analysis (%)			
Complex	C	H	N	m/z (M^+)
[Ga(tstach)]·2H_2O	59.15 (58.90)	5.90 (6.25)	7.50 (7.65)	513
[In(tstach)]	58.35 (57.95)	6.05 (5.40)	7.30 (7.50)	559
[Fe(tstach)]·0.5H_2O	63.60 (63.65)	6.15 (6.15)	8.20 (8.25)	500
[Ga(tnstach)]·H_2O	48.75 (48.80)	4.55 (4.40)	12.85 (12.65)	636
[In(tnstach)]·H_2O	45.85 (45.50)	4.45 (4.10)	11.65 (11.80)	695
[Fe(tnstach)]·H_2O	49.40 (49.60)	4.95 (4.50)	12.70 (12.85)	649
[Ga(tmstach)]·0.5H_2O	58.80 (58.75)	6.20 (6.10)	6.65 (6.85)	604
[In(tmstach)]·2H_2O	53.05 (52.55)	6.20 (5.90)	5.60 (6.15)	649
[Fe(tmstach)]·1.5H_2O	58.25 (58.35)	6.35 (6.40)	6.60 (6.80)	591

Table 2 Infrared spectral data (cm^{-1}) for the chelators and their complexes

Compound	ν(NH)		δ(NH)	δ(phenyl)
H_3tstach	3263s		1591s	1608m, 1471s
[Fe(tstach)]	3242w		1566w	1591m, 1477s
[Ga(tstach)]	3232m		1568w	1595m, 1475s
[In(tstach)]	3238w		1564w	1595m, 1477s
	ν(NH)	δ(NH)	δ(phenyl)	ν(NO_2)
H_3tnstach·3HCl	3000w (br)	1593s	1622m, 1496s	1496m, 1338s
[Fe(tnstach)]	3238w	1576m	1597m, 1477s	1491s, 1336s
[Ga(tnstach)]	3244w	1576m	1601m, 1481s	1482s, 1332s
[In(tnstach)]	3244w	1576m	1599m, 1477s	1491s, 1336s
	ν(NH)		ν(CH)	δ(phenyl)
H_3tmstach	3273s		2939m	1487s
[Fe(tmstach)]	3236m		2935m	1483s
[Ga(tmstach)]	3246m		2937m	1487s
[In(tmstach)]	3238m		2933m	1483s

Table 3 Absorption maxima and absorption coefficients for the complexes

Complex	λ_{max}/nm	10^{-4} ε/dm^3 mol^{-1} cm^{-1}
[Fe(tstach)]	460	0.19
	282	1.5
	238	1.5
[Ga(tstach)]	286	0.66
	244	2.1
[In(tstach)]	288	0.77
	250	1.6
[Fe(tnstach)]	500	0.30
	368	4.0
	240	1.7
[Ga(tnstach)]	366	4.6
	226	1.6
[In(tnstach)]	368	5.7
	234	1.5
[Fe(tmstach)]	484	0.35
	306	1.8
	236	1.8
[Ga(tmstach)]	306	0.50
	246	1.2
[In(tmstach)]	310	0.56
	254	1.0

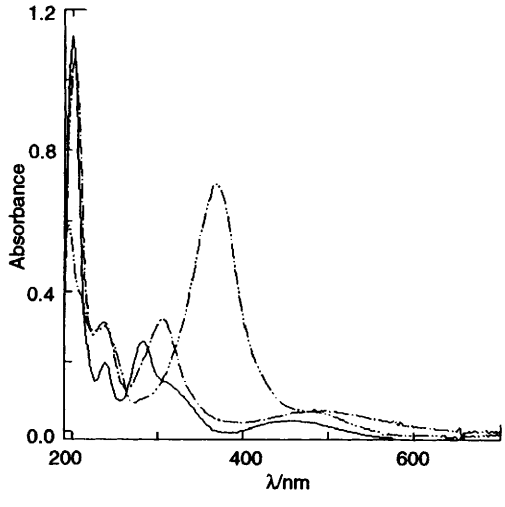

Fig. 1 Spectral overlay of the complexes [Fe(tstach)] (——), [Fe(tnstach)] (··——··) and [Fe(tmstach)] (—·—). Absorbances are adjusted such that the spectra are at equal solution concentrations

to a transition involving the iron(III) centre. This absorption band is observed at 460, 500 and 484 nm respectively for [Fe(tstach)], [Fe(tnstach)] and [Fe(tmstach)]. Since the absorption coefficients of this band are all approximately 10^3 dm^3 mol^{-1} cm^{-1} it is too intense to be due to a d–d transition, and is likely due to a ligand-to-metal charge-transfer (l.m.c.t.) transition. Observation of a long-wavelength l.m.c.t. absorption only for the iron(III) complexes is reasonable because this metal ion is the only one of the three that can undergo one-electron reduction at a low potential. Since these uncharged complexes have an N_3O_3 co-ordination sphere with three phenolate groups bonded to Fe^{III} it is likely that this l.m.c.t. transition is of the O→Fe^{III} type. The progression of the long-wavelength absorption bands partially supports this assignment (Fig. 1). The shift to longer wavelength of the 460 nm absorption band of [Fe(tstach)] to 484 nm for [Fe(tmstach)] results from the methoxy group being a stronger electron donor than hydrogen. The observation of an absorption band at 500 nm for [Fe(tnstach)] does not, however, support such a progression. Nevertheless, the comparison with this complex may not be valid because the l.m.c.t. band is very close in wavelength to the absorption band due to the nitro group, and therefore the

Table 4 Proton NMR [in $(CD_3)_2SO$ at ambient temperature] spectral data assignments for the chelators and their gallium and indium complexes

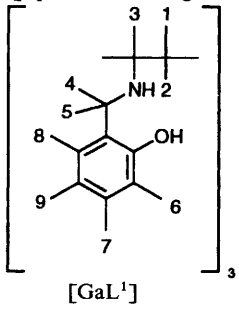

H_3tstach (H_3L^1)	H_3L^1·3HCl	[GaL^1]	[InL^1]	Assignment
0.89 (q, 3 H)[a]	1.77 (q, 3 H)[b]	1.65 (br d, 3 H)[c]	1.70 (br d, 3 H)[c]	H^1
2.19 (br d, 3 H)[a]	2.75 (br d, 3 H)[d]	2.32 (br d, 3 H)[c]	2.40 (br d, 3 H)[c]	H^2
2.42 (br s, 3 H)	3.23 (br s, 3 H)	3.01 (br s, 3 H)	3.08 (br s, 3 H)	H^3
		3.37 (br d, 3 H)[e]	3.27 (br d, 3 H)[e]	H^4
3.84 (s, 6 H)	4.07 (s, 6 H)			H^4 + H^5
		4.04 (br t, 3 H)[e]	4.23 (br t, 3 H)[e]	H^5
	6.97 (d, 3 H)[f]	6.12 (d, 3 H)[f]	6.27 (d, 3 H)[f]	H^6
6.67 (q, 6 H)[g]				H^6 + H^8
	7.45 (d, 3 H)[g]	6.90 (d, 4 H)[g]	6.89 (d, 3 H)[g]	H^8
	7.21 (t, 3 H)[f]	6.93 (t, 3 H)[f]	6.92 (t, 3 H)[f]	H^7
7.03 (t, 6 H)[g]				H^7 + H^9
	6.82 (t, 3 H)[g]	6.37 (t, 3 H)[g]	6.35 (t, 3 H)[g]	H^9
3–4 (br)	9.52 (br s, 6 H)	4.34 (br d, 3 H)	4.47 (m, 3 H)	NH
	10.30 (s, 3 H)	—	—	OH

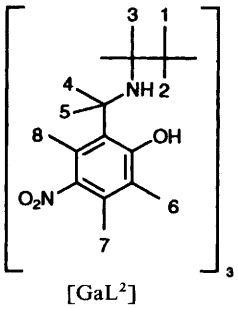

H_3tnstach(H_3L^2)	H_3L^2·3HCl	[GaL^2]	[InL^2]	Assignment
1.13 (m, 3 H)	1.8 (m, 3 H)	1.86 (br d, 3 H)[c]	1.89 (br d, 3 H)[h]	H^1
2.30 (m, 3 H)	2.74 (m, 3 H)	2.60 (br d, 3 H)[c]	2.56 (br d, 3 H)[h]	H^2
2.75 (m, 3 H)	3.33 (m, 3 H)	3.14 (br s, 3 H)	3.23 (br s, 3 H)	H^3
		3.37 (br d, 3 H)[a]	3.39 (br d, 3 H)[a]	H^4
3.95 (m, 6 H)	4.20 (s, 6 H)			H^4 + H^5
		4.24 (t, 3 H)[a]	4.37 (t, 3 H)[a]	H^5
6.54 (d, 3 H)[d]	7.18 (d, 3 H)[d]	6.26 (d, 3 H)[d]	6.48 (d, 3 H)[d]	H^6
7.91 (d, 3 H)[d]	8.18 (d, 3 H)[d]	7.96 (d, 3 H)[d]	7.96 (d, 3 H)[d]	H^7
8.04 (s, 3 H)	8.47 (s, 3 H)	7.95 (s, 3 H)	7.99 (s, 3 H)	H^8
4–6 (br)	9.65 (br s, 6 H)	5.58 (br d, 3 H)[i]	5.56 (br d, 3 H)[i]	NH
—	12.1 (br s, 3 H)	—	—	OH

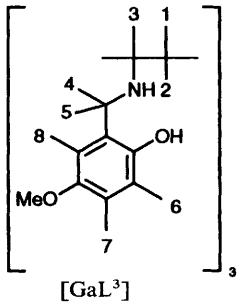

H_3tmstach(H_3L^3)	H_3L^3·3HCl	[GaL^3]	[InL^3]	Assignment
0.83 (q, 3 H)[b]	1.78 (q, 3 H)[b]	1.63 (br d, 3 H)[c]	1.66 (br d, 3 H)[h]	H^1
2.15 (br d, 3 H)[a]	2.77 (br d, 3 H)[j]	2.25 (br d, 3 H)[c]	2.35 (br d, 3 H)[h]	H^2
2.36 (m, 3 H)	3.21 (m, 3 H)	2.98 (br s, 3 H)	3.06 (br s, 3 H)	H^3
		3.36 (br d, 3 H)[a]	3.26 (br d, 3 H)[a]	H^4
3.78 (s, 6 H)	4.04 (s, 6 H)			H^4 + H^5
		3.95 (br t, 3 H)[a]	4.14 (br t, 3 H)[a]	H^5
6.56 (d, 3 H)	6.79 (d, 3 H)[f]	6.03 (d, 3 H)[f]	6.17 (d, 3 H)[f]	H^6
6.60 (d, 3 H)	6.88 (d, 3 H)[f]	6.56 (d, 3 H)[f]	6.55 (d, 3 H)[f]	H^7
6.65 (s, 3 H)	7.16 (s, 3 H)	6.55 (s, 3 H)	6.54 (s, 3 H)	H^8
—	9.62 (br s, 6 H)	4.18 (m, 3 H)	4.28 (m, 3 H)	NH
—	9.78 (s, 3 H)	—	—	OH
3.61 (s, 9 H)	3.67 (s, 9 H)	3.59 (s, 9 H)	3.58 (s, 9 H)	OMe

[a] ^2J(HH) = 11 Hz. [b] ^2J(HH) = 12 Hz. [c] ^2J(HH) = 15 Hz. [d] ^3J(HH) = 9 Hz. [e] ^2J(HH) = 10 Hz. [f] ^3J(HH) = 8 Hz. [g] ^3J(HH) = 7 Hz. [h] ^2J(HH) = 16 Hz. [i] ^3J(HH) = 11 Hz. [j] ^3J(HH) = 10 Hz.

overlapping of these bands makes the precise wavelength of λ_{max} for the l.m.c.t. transition more difficult to assign. Other phenolate and catecholate complexes of Fe^{III} are red.[61–63] Our assignment of the visible absorption band to a phenolate→iron(III) transition is supported by spectroscopic work on similar complexes which has led to the identification of such absorptions as $p_\pi \rightarrow d_{\pi^*}$ l.m.c.t. bands.[64] For the iron(III) complexes additional weak bands due to d–d transitions are expected. Our failure to observe such bands is due to their being obscured by the intense charge-transfer bands present.

The ^1H NMR spectra of the complexes (Table 4) are consistent with a six-co-ordinate structure. Complexation *via* the amine moiety is supported by the observation of an upfield shift in the NH resonance of 1–6 ppm for the complexes as compared to the free chelator. Complexation of the phenolate moiety is supported by the absence in the spectrum of any resonance due to a phenolic OH group. Another significant change between the ^1H NMR spectra of the complexes and chelators is observed in the methylenic protons. In both the free chelator and its hydrochloride salt, free rotation results in these protons H^4 and H^5 becoming magnetically equivalent (Table 4). In the diamagnetic complexes of Ga^{III} and In^{III}, however, chelation causes these protons to become inequivalent, and the two separate resonances are observed as a broad AB pair. The ^{13}C-{^1H} NMR spectra of these complexes show resonances that can be assigned to the different carbon atoms (Table 5).

The partition coefficients for the distribution of the complexes between octan-1-ol and water are large. From the data in Table 6, however, no particularly obvious trends emerge except that the complexes of tmstach consistently have the smallest values. This finding contrasts with our preconceived ideas that this compound with an alkoxy chain would yield complexes having the largest values. Possibly the higher hydrophobicity of the tnstach complexes is due to their having the lowest polarity of the group. For the complexes [M(tnstach)] both the nitro group and the trivalent metal ion are electron-withdrawing, thereby making the overall dipole moment of the complex lower than is obtained where the ligands do not have a nitro group appended to the periphery. For Ga^{III} none of the complexes has exceptionally large distribution coefficients, whereas the respective values of [Fe(tstach)] and [In(tnstach)] are large, 53 and 49.

The magnetic moments of the complexes all exhibit the high values characteristic of a high-spin complex in a weak ligand field. All three complexes show Curie–Weiss behaviour with a plot of $1/\chi$ against T extrapolating toward zero with a very small negative Weiss constant. The complexes therefore behave as isolated d^5 centres having weak antiferromagnetic couplings. As an example, [Fe(tnstach)] shows a linear fit for χ^{-1}/mol emu^{-1} against T/K with a Weiss constant θ of 0.6 K and a g value of 2.010. The magnetic susceptibility (μ) of this complex is 6.0 μ_B (*ca.* 55.6 × 10^{-23} J T^{-1}), which agrees with the spin-only value for an isolated metal ion with a spin $\frac{5}{2}$. Other phenolate and *N*,*N*′-bis(salicylidene)ethane-1,2-diamine (H_2salen) complexes of Fe^{III} are high spin. This is in agreement with our observation that the present ligands have a weak ligand field, even though we have been unable to confirm this by observing the d–d transitions in the iron complexes.[54]

The single-crystal structures of [M(tstach)]·xH_2O (x = 3, M = Fe; x = 3.5, M = Ga or In), [Fe(tnstach)] and

Table 5 ^{13}C-{^1H} NMR [in $(CD_3)_2SO$ at ambient temperature] spectral data assignments (δ) for the chelators and their gallium and indium complexes

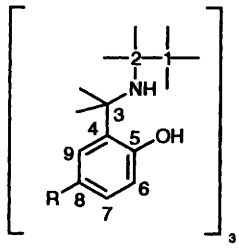

H_3L^1	[GaL^1]	[InL^1]	Assignment
38.8	30.6	30.2	C^1
52.8	53.5	53.9	C^2
48.4	53.0	53.0	C^3
124.6	126.3	125.6	C^4
158.2	166.0	166.8	C^5
118.8	120.0	120.6	C^6
128.2	128.7	129.5	C^7
115.9	114.5	114.1	C^8
128.7	129.2	130.0	C^9
H_3L^2	[GaL^2]	[InL^2]	Assignment
30.3	29.2	29.2	C^1
52.6	52.9	52.9	C^2
42.4	51.1	51.1	C^3
119.7	119.7	119.7	C^4
163.1	174.8	174.8	C^5
116.2	125.8	125.8	C^6
127.1	126.2	126.2	C^7
139.6	135.7	135.7	C^8
128.5	126.4	126.4	C^9
H_3L^3	[GaL^3]	[InL^3]	Assignment
38.9	30.8	30.3	C^1
48.3	53.1	53.1	C^2
52.9	53.5	53.9	C^3
125.5	126.2	125.4	C^4
152.1	159.6	160.7	C^5
116.2	119.8	120.4	C^6
113.1	114.6	115.1	C^7
151.7	149.8	149.0	C^8
114.4	114.6	115.7	C^9
55.7	55.8	55.9	OMe

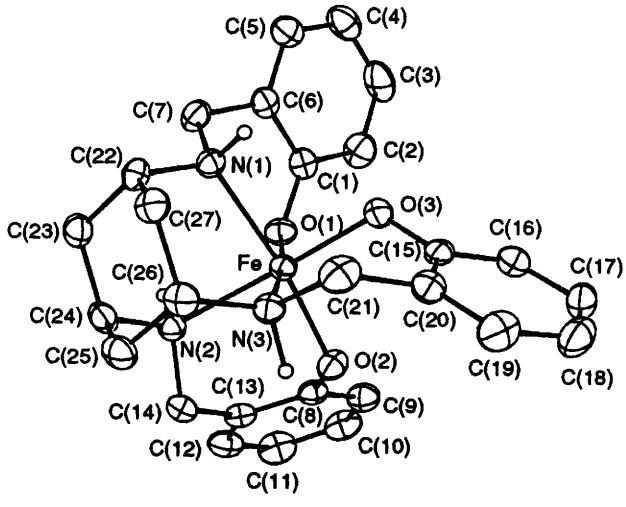

Fig. 2 An ORTEP representation of the structure of [Fe(tstach)]·$3H_2O$ with thermal ellipsoids at the 30% level

Table 6 Partition coefficients* for octanol–water for the complexes [ML]

	M		
L	Fe	Ga	In
tstach	53	13	14
tnstach	13	8.4	49
tmstach	4.8	5.2	9.6

* Defined as the concentration ratio in the two solvents.

Table 7 Selected crystallographic bond distances (Å) and angles (°)

Complex	M–N(1)	M–N(2)	M–N(3)	M–O(1)	M–O(2)	M–O(3)
[Fe(tstach)]	2.211(4)	2.222(4)	2.235(4)	1.936(4)	1.952(4)	1.909(4)
[Ga(tstach)]	2.147(2)	2.168(2)	2.128(2)	1.939(2)	1.909(2)	1.934(2)
[In(tstach)]	2.292(2)	2.305(2)	2.273(2)	2.114(2)	2.077(2)	2.102(2)
[Fe(tnstach)]	2.161(4)	2.225(4)	2.201(4)	1.943(3)	1.933(3)	1.920(3)
[Fe(tmstach)]	2.208(2)	2.255(2)	2.235(2)	1.926(2)	1.912(2)	1.926(2)

	trans-N–M–O	O–M–O	N–M–N
[Fe(tstach)]	172.6(2), 171.6(2), 172.8(2)	97.1(2), 96.5(2), 96.6(2)	87.0(2), 85.7(2), 86.0(2)
[Ga(tstach)]	174.82(8), 176.17(9), 175.74(8)	94.27(8), 94.77(8), 94.13(8)	88.14(9), 89.18(9), 87.58(9)
[In(tstach)]	171.50(7), 172.87(7), 172.55(7)	96.10(7), 97.23(7), 96.42(7)	86.38(8), 87.11(7), 85.99(7)
[Fe(tnstach)]	171.6(1), 175.4(2), 171.6(1)	97.7(1), 96.1(1), 92.8(1)	84.1(2), 86.9(2), 86.7(2)
[Fe(tmstach)]	168.21(8), 168.24(8), 170.42(8)	98.78(8), 100.10(8), 98.61(8)	84.01(9), 82.9(1), 84.98(9)

Table 8 Summary of crystallographic data *

Complex	[Ga(tstach)]·3.5H_2O	[In(tstach)]·3.5H_2O	[Fe(tstach)]·3H_2O	[Fe(tnstach)]·EtOH	[Fe(tmstach)]
Formula	$C_{27}H_{37}GaN_3O_6$	$C_{27}H_{37}InN_3O_{6.5}$	$C_{27}H_{36}FeN_3O_6$	$C_{29}H_{33}FeN_6O_{10}$	$C_{30}H_{36}FeN_3O_6$
M	577.39	622.49	554.45	681.53	590.48
Crystal size/mm	0.30 × 0.33 × 0.40	0.53 × 0.50 × 0.53	0.40 × 0.36 × 0.43	0.3 × 0.2 × 0.33	0.53 × 0.59 × 0.40
a/Å	15.062(1)	15.281(1)	15.210(2)	12.271(2)	13.737(1)
b/Å	11.372(1)	11.454(1)	11.386(1)	12.069(3)	7.676(1)
c/Å	15.2120(9)	15.338(1)	15.297(1)	20.540(2)	25.862(4)
β/°	93.464(6)	92.402(7)	93.197(7)	90.51(1)	92.18(1)
U/Å^3	2600.8(6)	2682.1(4)	2645.1(8)	3042(2)	2725(1)
D_c/g cm^{-3}	1.50	1.54	1.39	1.49	1.44
μ/cm^{-1}	11.0	9.15	6.121	5.58	5.99
Transmission factors	0.9475–0.9921	0.9499–1.0629	0.905–1.122	0.9256–0.9987	—
T/K	293	293	293	295	293
Scan range/°	0.80 + 0.34 tan θ	0.80 + 0.34 tan θ	0.80 + 0.34 tan θ	0.80 + 0.34 tan θ	0.80 + 0.30 tan θ
Total no. of reflections	5030	5187	5110	5925	5414
No. unique reflections	4576	4721	4651	5358	4788
R_{int}	0.019	0.015	0.038	0.045	0.021
No. observed data	3494 [$I \geqslant 3\sigma(I)$]	4074 [$I \geqslant 3\sigma(I)$]	2842 [$I \geqslant 2\sigma(I)$]	2672 [$I \geqslant 2\sigma(I)$]	3346 [$I \geqslant 3\sigma(I)$]
No. parameters	363	372	352	386	373
$(\Delta/\sigma)_{max}$ in last cycle	0.02	0.07	0.02	0.03	0.04
R	0.031	0.022	0.051	0.045	0.034
R'	0.044	0.035	0.070	0.049	0.047
Goodness of fit	1.49	1.33	2.00	1.27	1.57
Δρ in final Δ*F* map/e Å^3	0.80 to −0.67	0.28 to −0.10	0.93, −0.13	0.37, −0.15	0.42, −0.12

* Details in common: monoclinic, space group $P2_1/n$; $Z = 4$; graphite monochromated Mo-Kα radiation (λ 0.710 73 Å); ω–2θ scans; 2θ range, 1.0–50.0; $R = \Sigma||F_o| - |F_c||/\Sigma|F_o|$; $R' = [\Sigma w(||F_o| - |F_c||)^2/\Sigma w(|F_o|)^2]^{\frac{1}{2}}$ with $w = 1/(\sigma_F)^2$; $\sigma_F = \sigma(F^2)/2F$; $\sigma(F^2) = [(\sigma_I)^2 + (0.04F^2)^2]^{\frac{1}{2}}$; goodness of fit $= [\Sigma w(||F_o| - |F_c||)^2/(N_o - N_v)]^{\frac{1}{2}}$ where N_o and N_v are, respectively, the number of observations and variables.

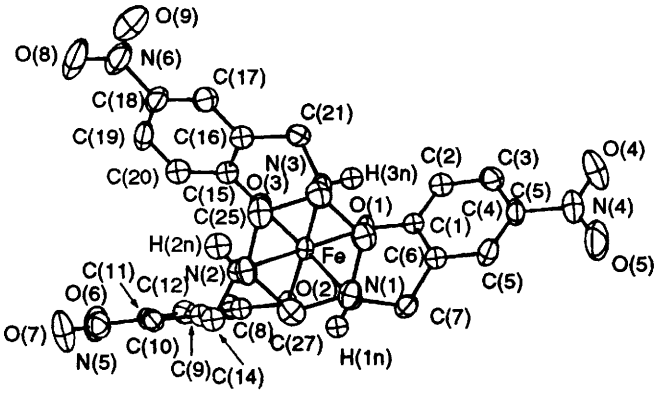

Fig. 3 An ORTEP representation of the structure of [Fe(tnstach)]·H_2O with thermal ellipsoids at the 30% level

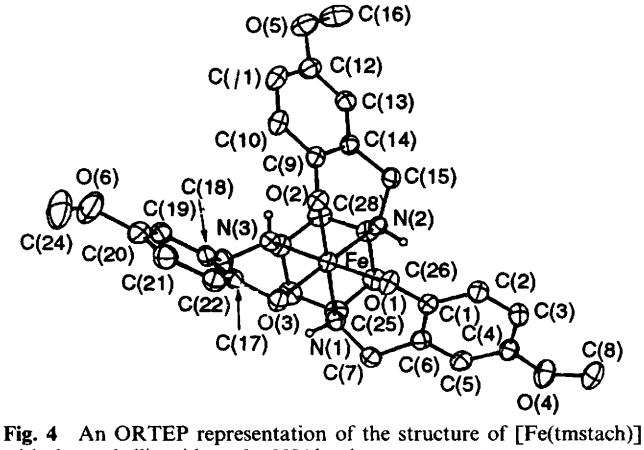

Fig. 4 An ORTEP representation of the structure of [Fe(tmstach)] with thermal ellipsoids at the 30% level

[Fe(tmstach)] confirm that in each case the co-ordination geometry about the central metal ion is octahedral with N_3O_3 ligating atoms (Figs. 2–6). No unusual bond distances or angles are found within the ligands, which suggests that the hexadentate co-ordination is achieved with minimal strain within the complex. In Table 7 are given selected bond distances and angles about the central metal ion. The average M–N bond

Table 9 Positional parameters for [Fe(tstach)]·3H_2O with estimated standard deviations in parentheses (e.s.d.s)

Atom	x	y	z	Atom	x	y	z
Fe	0.028 53(5)	0.206 13(6)	0.320 15(5)	C(14)	0.142 3(3)	0.289 4(5)	0.166 9(3)
O(1)	−0.057 2(2)	0.330 3(3)	0.300 2(2)	C(15)	0.070 6(3)	0.165 4(5)	0.498 8(3)
O(2)	0.130 6(2)	0.306 9(3)	0.345 7(2)	C(16)	0.080 6(4)	0.241 6(5)	0.569 8(4)
O(3)	0.003 5(2)	0.175 9(3)	0.439 0(2)	C(17)	0.149 1(4)	0.226 6(6)	0.633 3(4)
N(1)	−0.075 2(3)	0.079 5(4)	0.276 9(3)	C(18)	0.209 0(4)	0.135 2(6)	0.625 1(4)
N(2)	0.061 8(3)	0.217 5(4)	0.180 8(3)	C(19)	0.201 0(4)	0.061 6(5)	0.554 9(4)
N(3)	0.118 4(3)	0.050 8(4)	0.328 6(3)	C(20)	0.132 6(4)	0.074 7(5)	0.491 6(3)
C(1)	−0.134 1(3)	0.320 1(4)	0.339 7(3)	C(21)	0.119 5(4)	−0.009 1(5)	0.415 3(4)
C(2)	−0.161 6(4)	0.404 4(5)	0.398 4(4)	C(22)	−0.052 7(4)	−0.009 2(5)	0.211 1(3)
C(3)	−0.242 4(4)	0.391 7(6)	0.436 8(4)	C(23)	−0.026 4(4)	0.045 6(5)	0.125 8(3)
C(4)	−0.295 4(4)	0.295 8(6)	0.416 3(4)	C(24)	0.064 1(4)	0.104 1(5)	0.130 8(3)
C(5)	−0.268 9(4)	0.212 8(5)	0.358 5(4)	C(25)	0.133 6(4)	0.019 3(5)	0.169 8(4)
C(6)	−0.188 7(3)	0.223 7(5)	0.319 7(3)	C(26)	0.110 5(4)	−0.036 3(5)	0.255 9(4)
C(7)	−0.161 7(4)	0.137 0(5)	0.252 7(4)	C(27)	0.019 5(4)	−0.092 5(5)	0.247 6(4)
C(8)	0.132 5(3)	0.407 9(4)	0.301 9(3)	O(1s)	0.279 1(3)	0.308 2(4)	0.466 7(3)
C(9)	0.128 0(4)	0.515 8(5)	0.344 3(4)	O(2s)	0.567 8(6)	0.046 0(8)	0.273 8(6)
C(10)	0.134 0(4)	0.619 5(5)	0.298 5(4)	O(3s)	0.564 1(7)	0.046 (1)	0.456 6(7)
C(11)	0.143 3(4)	0.618 0(5)	0.209 8(4)	O(4s)	0.439 2(5)	0.184 3(7)	0.526 2(5)
C(12)	0.145 9(4)	0.511 4(5)	0.165 8(4)	O(5s)	0.425 7(6)	0.005 1(9)	0.669 7(8)
C(13)	0.139 4(3)	0.405 7(5)	0.210 8(4)				

Table 10 Positional parameters for [Fe(tnstach)]·H_2O with e.s.d.s in parantheses

Atom	x	y	z	Atom	x	y	z
Fe	0.147 97(5)	0.201 41(6)	0.216 29(3)	C(10)	0.203 9(4)	0.092 6(4)	0.004 7(2)
O(1)	0.232 3(2)	0.226 6(3)	0.295 4(1)	C(11)	0.311 7(4)	0.094 4(4)	−0.012 8(2)
O(2)	0.237 1(2)	0.084 8(3)	0.180 4(1)	C(12)	0.394 3(4)	0.093 8(4)	0.032 1(2)
O(3)	0.217 9(2)	0.313 9(3)	0.165 4(1)	C(13)	0.370 0(4)	0.091 5(4)	0.097 4(2)
O(4)	0.135 2(3)	0.279 3(4)	0.590 0(2)	C(14)	0.061 6(4)	0.081 3(4)	0.092 9(2)
O(5)	0.050 3(5)	0.128 8(4)	0.570 2(2)	C(15)	0.170 5(4)	0.395 1(4)	0.132 5(2)
O(6)	0.434 8(3)	0.096 2(4)	−0.097 6(2)	C(16)	0.092 0(4)	0.461 0(4)	0.161 7(2)
O(7)	0.263 8(3)	0.095 0(4)	−0.121 6(2)	C(17)	0.047 0(4)	0.548 3(4)	0.126 7(2)
O(8)	0.067 0(4)	0.680 7(4)	−0.027 4(2)	C(18)	0.081 2(4)	0.568 6(4)	0.064 0(2)
O(9)	−0.031 1(4)	0.720 8(4)	0.056 5(2)	C(19)	0.156 2(4)	0.503 4(5)	0.034 3(2)
N(1)	0.047 4(3)	0.082 4(3)	0.266 5(2)	C(20)	0.201 0(4)	0.416 0(5)	0.067 6(2)
N(2)	0.030 0(3)	0.176 2(3)	0.134 7(2)	C(21)	0.065 2(4)	0.445 1(4)	0.232 5(2)
N(3)	0.035 7(3)	0.329 5(3)	0.252 0(2)	C(22)	−0.072 8(4)	0.096 8(4)	0.266 2(2)
N(4)	0.104 8(4)	0.206 5(4)	0.553 0(2)	C(23)	−0.108 5(3)	0.207 9(4)	0.292 9(2)
N(5)	0.338 4(4)	0.094 9(4)	−0.082 7(2)	C(24)	−0.084 8(4)	0.306 2(4)	0.248 7(2)
N(6)	0.035 0(4)	0.662 1(4)	0.028 5(2)	C(25)	−0.122 3(4)	0.285 2(5)	0.179 0(2)
C(1)	0.198 7(3)	0.222 1(4)	0.357 1(2)	C(26)	−0.088 2(4)	0.174 4(4)	0.150 8(2)
C(2)	0.237 0(4)	0.299 8(5)	0.401 1(2)	C(27)	−0.116 5(4)	0.080 5(4)	0.197 1(2)
C(3)	0.205 5(4)	0.295 7(5)	0.465 9(2)	O(1s)	0.921 7(3)	0.143 8(3)	0.779 0(2)
C(4)	0.134 3(4)	0.213 1(4)	0.484 3(2)	C(1s)	0.972 9(5)	0.227 2(5)	0.739 2(3)
C(5)	0.094 9(4)	0.136 2(4)	0.441 1(2)	C(2s)	1.088 6(5)	0.235 2(6)	0.756 0(3)
C(6)	0.126 1(4)	0.140 5(4)	0.376 4(2)	H(1n)	0.060(3)	0.028(3)	0.243(2)
C(7)	0.094 5(4)	0.048 2(4)	0.330 5(2)	H(2n)	0.042(3)	0.234(4)	0.114(2)
C(8)	0.261 8(4)	0.088 3(4)	0.117 4(2)	H(3n)	0.048(3)	0.335(3)	0.289(2)
C(9)	0.177 2(4)	0.089 1(4)	0.070 2(2)	H(1o)	0.864(3)	0.163(3)	0.785(2)

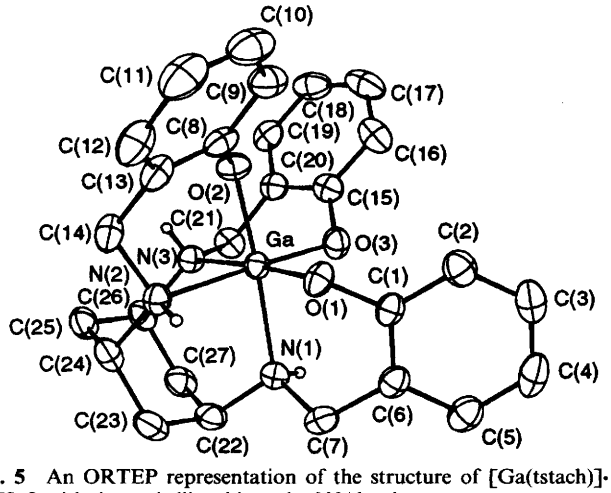

Fig. 5 An ORTEP representation of the structure of [Ga(tstach)]·3.5H_2O with thermal ellipsoids at the 30% level

distances range from 2.15 to 2.29 Å, with the gallium(III) complex having the shortest and that of In^{III} the longest. The average M–O distance ranges from 1.92 to 2.10 Å, with the longest being found for [In(tstach)]·3.5H_2O. The longer In–N and In–O distances are to be expected because of the larger ionic radius of the In^{3+} ion. The average Fe–O and Ga–O distances are identical at 1.92 and 1.93 Å, which is in agreement with the identical ionic radii of Fe^{3+} and Ga^{3+}. The average Ga–N distance is significantly shorter at 2.15 Å than are the Fe–N distances, which fall in the 2.20–2.23 Å range. This shortening is somewhat unexpected, but it may arise because Ga^{3+} is a closed electronic shell ion, whereas by contrast the d^5 Fe^{3+} ion has partially filled 3d orbitals. The bond angles in the complexes all follow a regular pattern: O–M–O (average) are obtuse and fall in the range 94.4(0.3)–99.2(0.8)°, whereas N–M–N are acute and fall in the range 84.0(1.0)–88.3(0.8)°. The *trans*-N–M–O angles are all somewhat smaller than 180°.

Table 11 Positional parameters for [Fe(tmstach)] with e.s.d.s in parentheses

Atom	*x*	*y*	*z*	Atom	*x*	*y*	*z*
Fe	0.198 88(3)	0.212 73(5)	−0.038 24(1)	C(13)	0.409 4(2)	0.242 1(4)	−0.180 5(1)
O(1)	0.254 3(1)	0.354 2(2)	0.016 88(7)	C(14)	0.359 0(2)	0.267 8(3)	−0.135 1(1)
O(2)	0.216 4(1)	0.369 2(2)	−0.094 64(7)	C(15)	0.407 3(2)	0.232 4(4)	−0.082 9(1)
O(3)	0.062 3(1)	0.252 5(2)	−0.028 68(7)	C(16)	0.505 0(3)	0.195 5(5)	−0.273 6(1)
O(4)	0.482 5(2)	0.159 8(3)	0.187 14(8)	C(17)	0.002 9(2)	0.281 8(4)	−0.070 5(1)
O(5)	0.413 1(2)	0.275 0(3)	−0.274 40(8)	C(18)	−0.001 7(2)	0.161 0(4)	−0.111 1(1)
O(6)	−0.177 3(2)	0.354 2(4)	−0.202 68(9)	C(19)	−0.062 1(2)	0.191 3(4)	−0.154 4(1)
N(1)	0.191 0(2)	−0.008 2(3)	0.0161 4(9)	C(20)	−0.120 2(2)	0.339 3(4)	−0.157 6(1)
N(2)	0.352 5(2)	0.118 6(3)	−0.048 19(8)	C(21)	−0.118 1(2)	0.456 9(4)	−0.117 3(1)
N(3)	0.157 7(2)	0.008 7(3)	−0.096 75(9)	C(22)	−0.056 0(2)	0.429 2(4)	−0.074 0(1)
C(1)	0.312 0(2)	0.305 8(3)	0.056 8(1)	C(23)	0.050 8(2)	−0.009 1(4)	−0.104 2(1)
C(2)	0.390 6(2)	0.408 2(4)	0.074 0(1)	C(24)	−0.244 9(3)	0.487 7(7)	−0.206 5(2)
C(3)	0.448 6(2)	0.364 7(4)	0.117 1(1)	C(25)	0.237 5(2)	−0.179 0(3)	0.004 3(1)
C(4)	0.429 6(2)	0.214 3(4)	0.143 8(1)	C(26)	0.346 4(2)	−0.163 7(4)	−0.004 5(1)
C(5)	0.353 4(2)	0.108 8(4)	0.126 8(1)	C(27)	0.370 7(2)	−0.071 2(4)	−0.054 4(1)
C(6)	0.294 1(2)	0.151 1(4)	0.084 2(1)	C(28)	0.314 3(2)	−0.149 5(4)	−0.100 4(1)
C(7)	0.203 6(2)	0.047 8(4)	0.070 8(1)	C(29)	0.205 0(2)	−0.166 5(4)	−0.093 5(1)
C(8)	0.536 9(2)	0.286 9(5)	0.214 7(1)	C(30)	0.185 1(2)	−0.259 2(4)	−0.042 5(1)
C(9)	0.265 8(2)	0.343 4(3)	−0.137 3(1)	H(1n)	0.134(2)	−0.028(3)	0.012 6(9)
C(10)	0.226 7(2)	0.393 0(4)	−0.185 7(1)	H(2n)	0.375(2)	0.150(3)	−0.017 4(8)
C(11)	0.277 2(2)	0.369 7(4)	−0.229 9(1)	H(3n)	0.176(1)	0.052(3)	−0.121 5(8)
C(12)	0.368 6(2)	0.291 9(4)	−0.227 8(1)				

Table 12 Positional parameters for [Ga(tstach)] $\cdot 3.5H_2O$ with e.s.d.s in parentheses

Atom	*x*	*y*	*z*	Atom	*x*	*y*	*z*
Ga	0.028 39(2)	0.198 73(2)	−0.183 80(2)	C(16)	−0.157 9(2)	0.405 6(3)	−0.104 1(2)
O(1)	0.129 4(1)	0.299 8(2)	−0.154 0(1)	C(17)	−0.237 9(2)	0.395 7(3)	−0.064 2(2)
O(2)	0.000 7(1)	0.174 9(2)	−0.064 3(1)	C(18)	−0.292 0(2)	0.301 1(3)	−0.081 0(2)
O(3)	−0.055 1(1)	0.326 8(2)	−0.202 9(1)	C(19)	−0.267 6(2)	0.214 4(3)	−0.138 4(2)
N(1)	0.059 3(1)	0.212 9(2)	−0.319 3(1)	C(20)	−0.187 7(2)	0.222 5(2)	−0.179 1(2)
N(2)	0.118 5(1)	0.050 2(2)	−0.171 9(1)	C(21)	−0.161 8(2)	0.134 8(3)	−0.245 9(2)
N(3)	−0.074 3(1)	0.077 2(2)	−0.221 6(1)	C(22)	0.062 3(2)	0.100 7(3)	−0.370 3(2)
C(1)	0.131 2(2)	0.403 2(2)	−0.197 3(2)	C(23)	0.133 5(2)	0.016 7(3)	−0.331 7(2)
C(2)	0.126 7(2)	0.510 2(3)	−0.153 1(2)	C(24)	0.111 3(2)	−0.038 8(2)	−0.244 8(2)
C(3)	0.132 9(2)	0.614 6(3)	−0.197 5(2)	C(25)	0.019 5(2)	−0.095 8(2)	−0.252 4(2)
C(4)	0.143 2(2)	0.615 2(3)	−0.287 5(2)	C(26)	−0.054 2(2)	−0.014 2(3)	−0.288 3(2)
C(5)	0.144 9(2)	0.509 4(3)	−0.333 0(2)	C(27)	−0.029 0(2)	0.041 0(3)	−0.374 9(2)
C(6)	0.138 0(2)	0.402 9(3)	−0.288 6(2)	O(1s)	−0.221 1(2)	0.193 4(2)	0.466 0(2)
C(7)	0.139 9(2)	0.286 7(3)	−0.333 7(2)	O(2s)	−0.072 9(2)	0.517 5(3)	−0.304 9(3)
C(8)	0.068 3(2)	0.167 0(3)	−0.003 5(2)	O(3s)	0.059 8(3)	0.687 6(3)	−0.527 1(3)
C(9)	0.076 6(2)	0.246 5(3)	0.066 8(2)	O(4s)	−0.065 8(4)	0.538 2(6)	−0.459 8(4)
C(10)	0.145 4(2)	0.232 5(3)	0.131 3(2)	H(1n)	0.018(2)	0.252(2)	−0.343(2)
C(11)	0.206 5(2)	0.143 9(3)	0.126 5(2)	H(2n)	0.171(2)	0.085(2)	−0.172(2)
C(12)	0.199 3(2)	0.066 4(3)	0.056 2(2)	H(3n)	−0.086(2)	0.040(3)	−0.181(2)
C(13)	0.131 2(2)	0.077 3(3)	−0.008 8(2)	H(1sa)	−0.265(2)	0.195(3)	0.430(2)
C(14)	0.119 2(2)	−0.008 2(3)	−0.083 5(2)	H(1sb)	−0.240(3)	0.207(4)	0.516(3)
C(15)	−0.131 9(2)	0.318 7(3)	−0.161 5(2)				

An important aspect of complexes of gallium to be used for *in vivo* imaging purposes is that they should be stable to replacement by other metal ions. One such metal ion that is common in an *in vivo* environment is Fe^{III}. Since the iron(III) complex [Fe(tstach)] is red due to an absorption band at 460 nm, and the analogous gallium(III) complex is colourless, we have tested this inertness by adding an excess of iron(III) ion to a colourless aqueous solution of [Ga(tstach)]. After 7 d no red colouration is observed, verifying that there is no formation of the complex [Fe(tstach)].

Preliminary in vivo *Studies with* ^{59}Fe.—The potential for use of these chelators and complexes as imaging or iron-sequestering agents is presently under investigation *in vivo* using radioactive $^{59}Fe^{III}$ and $^{67}Ga^{III}$ in mice. Preliminary results show that the radioactive iron complex of each chelator is cleared rapidly from the bloodstream as compared to uncomplexed Fe^{III}, with [^{59}Fe(tnstach)] being the slowest. Despite rapid clearance, [^{59}Fe(tnstach)] shows a different pattern of selective tissue uptake when compared to transferrin-bound iron. Over 2 h [^{59}Fe(tnstach)] enhances uptake into lung, skin, adrenal, liver and kidney tissues, while diminishing spleen, bone and brain uptake. Over longer periods the differences of uptake in various tissues begin to match more closely the uptake of the non-complexed iron control group, implying that metabolism of the complexes releases free iron, possibly by protonation of the phenolate functionalities of the ligand.[65] Full details of these *in vivo* experiments are being published elsewhere.[66]

Acknowledgements

We thank the Center for Bioenvironmental Research and the Veterans Administration for financial support.

Table 13 Positional parameters for [In(tstach)]·3.5H_2O with e.s.d.s in parntheses

Atom	*x*	*y*	*z*	Atom	*x*	*y*	*z*
In	0.029 01(1)	0.210 08(1)	−0.177 09(1)	C(16)	−0.172 8(2)	0.407 8(2)	−0.100 4(2)
O(1)	0.138 8(1)	0.318 9(1)	−0.151 5(1)	C(17)	−0.251 8(2)	0.391 2(3)	−0.062 5(2)
O(2)	0.003 3(1)	0.178 1(2)	−0.047 4(1)	C(18)	−0.301 4(2)	0.293 3(2)	−0.081 9(2)
O(3)	−0.064 2(1)	0.343 5(1)	−0.196 8(1)	C(19)	−0.271 2(2)	0.212 1(2)	−0.139 8(2)
N(1)	0.064 6(1)	0.222 4(2)	−0.320 5(1)	C(20)	−0.191 3(1)	0.227 6(2)	−0.179 2(1)
N(2)	0.120 3(1)	0.049 9(2)	−0.168 4(1)	C(21)	−0.161 7(1)	0.143 1(2)	−0.247 1(1)
N(3)	−0.077 7(1)	0.082 3(2)	−0.221 3(1)	C(22)	0.066 4(2)	0.108 2(2)	−0.368 1(1)
C(1)	0.138 0(1)	0.416 6(2)	−0.198 5(1)	C(23)	0.134 6(2)	0.024 1(2)	−0.328 1(2)
C(2)	0.132 1(2)	0.526 0(2)	−0.158 4(2)	C(24)	0.110 6(2)	−0.033 2(2)	−0.243 1(2)
C(3)	0.134 9(2)	0.626 6(2)	−0.208 1(2)	C(25)	0.018 2(2)	−0.086 3(2)	−0.250 8(2)
C(4)	0.142 8(2)	0.622 0(2)	−0.296 6(2)	C(26)	−0.052 7(1)	−0.005 4(2)	−0.287 3(1)
C(5)	0.145 8(2)	0.513 4(2)	−0.337 7(2)	C(27)	−0.024 4(2)	0.051 6(2)	−0.372 2(1)
C(6)	0.142 7(1)	0.410 4(2)	−0.290 1(1)	O(1s)	−0.218 7(1)	0.187 7(2)	0.469 9(1)
C(7)	0.146 0(2)	0.292 6(2)	−0.332 2(2)	O(2s)	−0.066 5(2)	0.551 3(3)	0.726 3(2)
C(8)	0.073 2(1)	0.164 0(2)	0.006 6(1)	O(3s)	−0.060 8(2)	0.315 0(3)	0.529 9(2)
C(9)	0.086 4(2)	0.237 5(2)	0.078 5(2)	O(4s)	−0.064 3(3)	0.543 8(5)	0.545 7(3)
C(10)	0.157 3(2)	0.219 6(3)	0.137 1(2)	O(5s)	−0.075 3(3)	0.488 9(5)	0.665 4(4)
C(11)	0.215 6(2)	0.129 4(3)	0.124 8(2)	H(1n)	0.030(1)	0.254(2)	−0.343(1)
C(12)	0.203 8(2)	0.058 0(2)	0.053 0(2)	H(2n)	0.161(1)	0.075(2)	−0.169(1)
C(13)	0.133 1(2)	0.073 1(2)	−0.006 5(1)	H(3n)	−0.085(1)	0.054(2)	−0.185(1)
C(14)	0.117 4(2)	−0.008 9(2)	−0.081 9(2)	H(1sa)	−0.257(2)	0.189(2)	0.431(2)
C(15)	−0.141 2(1)	0.3263(2)	−0.158 8(1)	H(1sb)	−0.247(2)	0.198(3)	0.512(2)

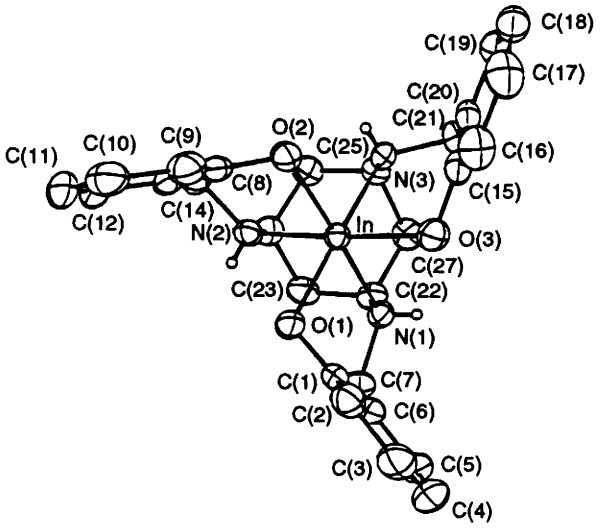

Fig. 6 An ORTEP representation of the structure of [In(tstach)]·3.5H_2O with thermal ellipsoids at the 30% level

References

1 R. C. Hider and A. D. Hall, *Prog. Med. Chem.*, 1991, **28**, 41.
2 H. R. Hoveyda, V. Karunaratne, S. J. Rettig and C. Orvig, *Inorg. Chem.*, 1992, **31**, 5408.
3 D. A. Moore, P. E. Fanwick and M. J. Welch, *Inorg. Chem.*, 1989, **28**, 1504.
4 S. M. Moerlein, M. J. Welch, K. N. Raymond and F. L. Weitl, *J. Nucl. Med.*, 1981, **22**, 710.
5 C. J. Mathias, Y. Sun, M. J. Welch, M. A. Green, J. A. Thomas, K. R. Wade and A. E. Martell, *Nucl. Med. Biol.*, 1988, **15**, 69.
6 V. L. Alvarez, M. L. Wen, C. Lee, A. D. Lopes, J. D. Rodwell and T. J. McKearn, *Nucl. Med. Biol.*, 1986, **13**, 347.
7 M. Koizumi, K. Endo, M. Kunimatsu, H. Sakahara, T. Nakashima, Y. Kawamura, Y. Watanabe, Y. Ohmomo and Y. Arano, *J. Immunol. Methods*, 1987, **104**, 93.
8 C. Loc'h, B. Maziere and D. Comar, *J. Nucl. Med.*, 1980, **21**, 171.
9 R. J. Motekaitis, A. E. Martell and M. J. Welch, *Inorg. Chem.*, 1994, **33**, 1241.
10 A. J. Carty and D. G. Tuck, *Prog. Inorg. Chem.*, 1975, **19**, 245.
11 I. A. Sheka, I. S. Chaus and T. T. Mityureva, *The Chemistry of Gallium*, Elsevier, New York, 1966.
12 M. J. Taylor, *Comprehensive Coordination Chemistry*, ed. G. Wilkinson, Pergamon, Oxford 1987, vol. 3, Ch. 25.1.
13 D. G. Tuck, *Pure Appl. Chem.*, 1983, **55**, 1477.
14 D. A. Betebenner, P. L. Carney, A. M. Zimmer, J. M. Kazikiewicz, E. Brücher, A. D. Sherry and D. K. Johnson, *Bioconjugate Chem.*, 1991, **2**, 117.
15 S. Jurisson, D. Benning, W. Jia and D. Ma, *Chem. Rev.*, 1993, **93**, 1137.
16 A. N. Serafini, R. Vargas-Cuba, P. Benedetto, A. Legaspi, L. Feun, D. Robinson, B. Ardalan, M. K. Dewanjee, B. U. Sevin, H. Averette and G. Sfakianakis, *Antibody, Immunoconjugates Radiopharm.*, 1991, **4**, 77.
17 A. N. Serafini, I. Garty, R. Vargas-Cuba, A. Friedman, D. A. Rauh, M. Neptune, L. Landress and G. N. Sfakianakis, *J. Nucl. Med.*, 1991, **32**, 2227.
18 I. Ogihara-Umeda, T. Sasaki and H. Nishigori, *Nucl. Med. Biol.*, 1992, **19B**, 753.
19 O. A. Gansow, *Nucl. Med. Biol.*, 1991, **18B**, 369.
20 D. Parker, *Chem. Soc. Rev.*, 1990, **19**, 271.
21 M. W. Brechbiel, O. A. Gansow, R. W. Atcher, J. Schlom, J. Esteban, D. E. Simpson and D. Colcher, *Inorg. Chem.*, 1986, **25**, 2772.
22 S. V. Deshpande, R. Subramanian, M. J. McCall, S. J. DeNardo, G. L. DeNardo and C. F. Meares, *J. Nucl. Med.*, 1990, **31**, 218.
23 A. Evers, R. D. Hancock, A. E. Martell and R. J. Motekaitis, *Inorg. Chem.*, 1989, **28**, 2189.
24 A. S. Craig, D. Parker, H. Adams and N. A. Bailey, *J. Chem. Soc., Chem. Commun*, 1989, 1793.
25 A. S. Craig, I. M. Helps, K. J. Jankowski, D. Parker, N. R. A. Beeley, B. A. Boyce, M. A. W. Eaton, A. T. Millican, K. Millar, A. Phipps, S. K. Rhind, A. Harrison and C. Walker, *J. Chem. Soc., Chem. Commun.*, 1989, 794.
26 G. A. Sumerdon, P. E. Rogers, C. M. Lombardo, K. E. Schnolrich, S. L. Melvin, E. D. Hobart, I. I. E. Tribby, S. D. Stroupe and D. K. Johnson, *Nucl. Med. Biol.*, 1990, **17B**, 247.
27 C. Wu, F. Virzi and D. J. Hnatowich, *Nucl. Med. Biol.*, 1992, **19B**, 239.
28 L. C. Washburn, L. D. Blair, B. L. Byrd and T. T. Sun, *Int. J. Nucl. Med. Biol.*, 1985, **12**, 267.
29 M. A. Green, C. J. Mathias, W. L. Newman, P. E. Fanwick, M. Janik and E. A. Deutsch, *J. Nucl. Med.*, 1993, **34**, 228.
30 B. W. Tsang, C. J. Mathias and M. A. Green, *J. Nucl. Med.*, 1993, **34**, 1127.
31 R. J. Motekaitis, A. E. Martell and M. J. Welch, *Inorg. Chem.*, 1990, **29**, 1463.
32 S. L. Madsen, M. J. Welch, R. J. Motekaitis and A. E. Martell, *Nucl. Med. Biol.*, 1992, **19B**, 431.
33 M. Zöller, J. Schuhmacher, J. Reed, W. Maier-Borst and D. Matzku, *J. Nucl. Med.*, 1992, **33**, 1366.
34 Z. Zhang, D. M. Lyster, G. A. Webb and C. Orvig, *Nucl. Med. Biol.*, 1992, **19B**, 327.

35 M. M. Finnegan, T. G. Lutz, W. O. Nelson, A. Smith and C. Orvig, *Inorg. Chem.*, 1987, **26**, 2171.
36 W. O. Nelson, T. B. Karpishin, S. J. Rettig and C. Orvig, *Inorg. Chem.*, 1988, **27**, 1045.
37 S. L. Madsen, C. J. Bannochie, A. E. Martell, C. J. Mathias and M. J. Welch, *J. Nucl. Med.*, 1990, **31**, 1662.
38 C. A. Matsuba, W. O. Nelson, S. J. Rettig and C. Orvig, *Inorg. Chem.*, 1988, **27**, 3935.
39 W. O. Nelson, T. B. Karpishin, S. J. Rettig and C. Orvig, *Can. J. Chem.*, 1988, **66**, 123.
40 C. J. Mathias, F. Sun, J. M. Connett, G. W. Philpott, M. J. Welch and A. E. Martell, *Inorg. Chem.*, 1990, **29**, 1475.
41 J. E. Bollinger, J. T. Mague and D. M. Roundhill, *Inorg. Chem.*, 1994, **33**, 1241.
42 R. D. A. Wentworth and J. J. Felten, *J. Am. Chem. Soc.*, 1968, **90**, 621.
43 U. Brand and H. Vahrenkamp, *Inorg. Chim. Acta*, 1992, **198–200**, 663.
44 K. Hegetschweiler, M. Ghisletta, T. F. Fässler, R. Nesper, H. W. Schmalle and G. Rihs, *Inorg. Chem.*, 1993, **32**, 2032.
45 D. A. Moore, P. E. Fanwick and M. J. Welch, *Inorg. Chem.* 1990, **29**, 672.
46 S. Liu, E. Wong, S. J. Rettig and C. Orvig, *Inorg. Chem.*, 1993, **32**, 4268.
47 S. Liu, L. Gelmini, S. J. Rettig, R. C. Thompson and C. Orvig, *J. Am. Chem. Soc.* 1992, **114**, 6081.
48 M. A. Green, C. J. Mathias, W. L. Neumann, P. E. Fanwick, M. Janik and E. A. Deutsch, *J. Nucl. Med.*, 1993, **34**, 228.
49 C. Hershko, (Editor), *Baillière's Clinical Haematology*, Ballière Tindall, London, 1989, vol. 2.
50 A. E. Martell, R. J. Motekaitis, I. Murase, L. F. Sala, R. Stoldt, C. Y. Ng, H. Rosenkrantz and J. J. Metterville, *Inorg. Chim. Acta*, 1987, **138**, 215.
51 T. M. Garrett, T. J. McMurry, M. W. Hosseini, Z. E. Reyes, F. E. Hahn and K. N. Raymond, *J. Am. Chem. Soc.*, 1991, **113**, 2965.
52 T. B. Karpishin, M. S. Gebhard, E. I. Solomon and K. N. Raymond, *J. Am. Chem. Soc.*, 1991, **113**, 2977.
53 E. B. Fleischer, A. E. Gebala, A. Levey and P. A. Tasker, *J. Org. Chem.*, 1971, **36**, 3042.
54 D. A. Rudman, J. C. Huffman, R. F. Childers, W. E. Streib and R. A. D. Wentworth, *Inorg. Chem.*, 1975, **14**, 747.
55 C. J. O'Connor, *Prog. Inorg. Chem.*, 1979, **29**, 204.
56 J. T. Mague and C. L. Lloyd, *Organometallics*, 1988, **7**, 983.
57 MOLEN, An Interactive Structure Solution Procedure, Enraf-Nonius, Delft, 1990.
58 D. T. Cromer and J. T. Waber, *International Tables for X-Ray Crystallography*, Kynoch Press, Birmingham, 1974, vol. 4, Table 2.2B.
59 D. T. Cromer and J. T. Waber, *International Tables for X-Ray Crystallography*, Kynoch Press, Birmingham, 1974, vol. 4, Table 3.2.1.
60 C. K. Johnson, ORTEP, Report ORNL-5138, Oak Ridge National Laboratory, Oak Ridge, TN, 1976.
61 S. A. Koch and M. Millar, *J. Am. Chem. Soc.*, 1982, **104**, 5255.
62 R. H. Heistand II, R. B. Lauffer, E. Fikrig and L. Que, jun., *J. Am. Chem. Soc.*, 1982, **104**, 2789.
63 K. N. Raymond, S. S. Isied, L. D. Brown, F. R. Fronczek and J. H. Nibert, *J. Am. Chem. Soc.*, 1976, **98**, 1767.
64 B. P. Gaber, V. Miskowski and T. G. Spiro, *J. Am. Chem. Soc.*, 1974, **96**, 6868.
65 E. Cole, R. C. B. Copley, J. A. K. Howard, D. Parker, G. Ferguson, J. F. Gallagher, B. Kaitner, A. Harrison and L. Royle, *J. Chem. Soc., Dalton Trans.*, 1994, 1619.
66 J. E. Bollinger, W. A. Banks, A. J. Kastin and D. M. Roundhill, unpublished work.

Received 22*nd December* 1994; *Paper* 4/07810A